water

MDPI

*Article*

# Model Based Assessment of the Reflection Behavior of Tidal Waves at Bathymetric Changes in Estuaries

**Vanessa Sohrt [1,*], Sebastian S.V. Hein [2], Edgar Nehlsen [1], Thomas Strotmann [2] and Peter Fröhle [1]**

[1] Institute of River and Coastal Engineering, Hamburg University of Technology, 21073 Hamburg, Germany; nehlsen@tuhh.de (E.N.); froehle@tuhh.de (P.F.)
[2] Hamburg Port Authority, Hydrology, 20457 Hamburg, Germany; Sebastian.Hein@hpa.hamburg.de (S.S.V.H.); Thomas.Strotmann@hpa.hamburg.de (T.S.)
* Correspondence: vanessa.sohrt@tuhh.de

**Abstract:** Estuaries are often modified by human activities. Adjustments in the morphology of an estuary have a potential impact on the hydrodynamics and on the reflection behavior of the tide. The influence of such system changes on the complex tidal regime with a large number of superimposed tidal constituents is not fully understood yet. The reflection properties of estuaries that are characterized by abrupt changes in geometry are systematically investigated on the basis of simplified estuary model approaches to improve the understanding of the oscillation and reflection behavior of tidal waves in estuaries. The reflection coefficients at abrupt cross-sectional changes are determined by two different methods, i.e., an analytical energy-based approach and a hydrodynamic numerical (HN) model. Comparisons indicate a high agreement of the results of the different methods when evaluating the reflection coefficient. The tidal constituents are reflected at partial and total reflectors and amplified by shoaling depending on the water depths, the height of the bottom step and the horizontal constriction. A harmonic analysis of simulated water level data partly shows the formation and amplification of higher harmonic components as a result of shallow water effects. The interaction with reflectors results in an increasing amplification of the tidal constituents and the tide.

**Keywords:** reflection; tidal wave; estuaries; model; analytical; hydrodynamic numerical modelling



**Citation:** Sohrt, V.; Hein, S.S.V.; Nehlsen, E.; Strotmann, T.; Fröhle, P. Model Based Assessment of the Reflection Behavior of Tidal Waves at Bathymetric Changes in Estuaries. *Water* **2021**, *13*, 489. https://doi.org/10.3390/w13040489

Academic Editor: Yakun Guo

Received: 20 December 2020
Accepted: 8 February 2021
Published: 13 February 2021



## 1. Introduction

Estuaries are often modified by human activities for various purposes, such as to improve their navigability or flood protection. This includes the construction of storm surge barriers on tributary rivers, dikes, and other flood protection measures as well as the construction of ports or the repeated adjustments (deepening) of navigation channels (fairways) to ports. These changes in the morphology of estuaries lead to changes in the current and the water level conditions, and thus to a change of the tidal wave in estuaries. The main navigation channel in estuaries is deepened, widened, and more or less channelized. This will reduce the damping effects on the tidal wave, resulting in a less damped incoming tidal wave with higher local tidal range [1,2]. The shoaling of the tidal wave leads to an increase of the tidal range, and in addition, in estuaries possibly occurring abrupt geometric changes (bottom steps, widening/narrowing of the cross section, etc. [3]) lead to a (partial) reflection of the incoming tidal wave, which also increases the tidal range. The influence of system changes on the complex tidal regime in estuaries, where a large number of tidal constituents are superimposed, is not fully understood yet.

For wind-induced, short-period waves, there are many approaches to determine the reflection coefficients of reflectors. These include techniques to resolve the incident and reflected waves from the records of composite waves from different number of gauges (e.g., Goda and Suzuki [4], Mansard and Funke [5], Baldock and Simmonds [6], Brossard et al. [7]). Given that an application of the aforementioned gauge methods on measured data is not reasonable without an extension by the consideration of re-reflection and the consideration

of a degree of dissipation, they will be left out in the following discussion. In addition, there are empirical methods to assess the reflection coefficient for data generated in the laboratory (e.g., Davidson et al. [8], Renouard et al. [9], Sutherland and O'Donoghue [10], Wiegel [11]). The approaches that include the calculation of the reflection potential of short-period waves with an empirical formulation are not suitable for estimating the reflection behavior of long-period tidal waves and will not be considered further, as the determination of the reflection coefficient is based on the theory of short waves.

There are also a variety of analytical models to calculate the tidal wave propagation in an estuary (among others Hunt [12], Dronkers [13], Prandle and Rahman [14], Friedrichs and Aubrey [15], Lanzoni and Seminara [16], Savenije [17], and van Rijn [18]). The reflection in these models is usually only considered in the equations including one reflector at the landward end. In the case of van Rijn, the analytical model that takes reflection processes into account produces amplification values that are "too large" [18] in comparison to observed tidal ranges (a specification, which values are obtained or to which extent the calculated amplification is too large, is missing) and are not shown in the publication [18]. These analytical models, which in most cases include total reflection and are often based on the continuity and momentum equations, will not be considered further in the following because the specification of a reflection coefficient is missing.

In addition, there are approaches (as for example, according to Lamb [19] and Dean and Dalrymple [20]) where the reflection coefficient calculation is based on the boundary considerations that (i) any finite water level change over an infinitely small distance would give rise to infinite accelerations of the fluid particles, so that the water levels on each side of the step should be the same (long wave equations of motion [20], or continuity of pressure [19]) and (ii) the mass flow rates from regions located upstream and downstream of abrupt bathymetric change are equal to another (continuity consideration). Since condition (i) is valid only for long periodic waves, it is expected that the calculations of the reflection coefficient according to Lamb [19] and Dean and Dalrymple [20] can lead to realistic estimates of the reflection coefficient for tidal waves.

Lin [21] conducted numerical reflection investigations of solitary waves at rectangular obstacles. The numerical investigations showed a high agreement (for weakly nonlinear waves, i.e., wave height $H$ to water depth $h$ ratio = 0.1, and under the consideration of dissipation) with the results from Lamb [19] for the case of a very long obstacle (the ratio between the length of the obstacle and the water depth is 70). Up to an obstacle height/water depth ratio of 0.85, the relative deviation is 10% (beyond that ratio up to 32%). For shorter obstacle lengths, a significant deviation from the numerical results to the solution of Lamb was found.

Le Cann [22] set up a numerical model of the Bay of Biscay to investigate the tidal dynamics of the tidal components of $M_2$ and $M_4$ and their variability in the shelf. In his studies the $M_2$ amplitude is increasing the cross shore by an order of 20% with its maximum at the shelf break. Between the shelf break and the coast, the $M_4$ amplitudes are increasing by a factor of 10, indicating resonance in the central part of the shelf. Le Cann derived the mean energy fluxes and dissipation of the $M_2$ component from the numerical model results and compared these results with the energy fluxes obtained from measured data. The comparison showed similar results for both tidal constituents $M_2$ and $M_4$ in direction and amplitude. Le Cann provided possible shallow water partial tide $M_4$ generating terms and its approximate magnitudes in the nonlinear moment and continuity equations. The generation of quarter diurnal components due to the nonlinear shallow water equations of motion and continuity was also described in Pingree et al. [23].

Díez-Minguito et al. [24] were probably the first to analyze tidal wave reflection in the Guadalquivir Estuary at the Alcalá del Río head dam based on measured data [24]. They determined a frequency dependent "complex reflection coefficient" and applied the observations to the sedimentation behavior in the estuary. The analysis of tidal reflection is based on a gauges method of Baquerizo [25] using a least squares fitting technique. This method is, according to Díez-Minguito et al. [24] and [26], based on Mansard and Funke [5]

and is valid for the assumption that the same wave (with corresponding amplitude, length and phase) does not change between the gauges. Therefore, the width and depth of the channel need to be constant, and the dissipation due to friction with the bottom and margins is neglected. Water level data at three different gauges were used to separate the incident and reflected wave signals. The calculated reflection coefficient for the $M_2$ tidal constituent was 0.4, which is significantly less than 1.0, which is the expected value for a total reflector. It is assumed that this is a result of the dissipation and re-reflection, which is not considered.

In 2016, Díez-Minguito et al. [3] derived a qualitative criterion at which length scale of the bathymetric change the energy loss due to reflection becomes negligible. According to the authors, "If the length scale of the spatial changes in section is much larger than the tidal wavelength, energy losses due to reflection are negligible" [3].

To better understand the oscillation and reflection behavior of tidal waves in estuaries, the reflection coefficients of abrupt bathymetric changes are systematically investigated in this study. An energy-based approach to calculate the reflection coefficient at abrupt bathymetric changes is compared to the results of a hydrodynamic numerical model. A harmonic analysis is applied to simulation data of multiple wave signals, and the generation of higher-harmonic components is observed.

Tidal waves in an estuary deform because of various influences (headwater discharge, bed conditions, structures, etc.) while moving upstream from the river mouth. Tidal waves reflect at riverbed steps, bends, widenings, ramifications, structures, islands, and weirs. Abrupt bathymetric changes and artificially created tidal borders (e.g., a weir) are assumed to be the main reflection points. Tidal waves in general have a small wave steepness, and so the linear relation between the wave harmonic signals and nonlinear terms can be ignored. Therefore, tidal waves that are superimposed of several tidal constituents are assumed to be regular waves, which can get estimated through the linear wave theory. The focus of this paper is the investigation of the reflectance of tidal waves at abrupt bathymetric changes, since total reflections are already well understood, e.g., in respective literature as [2,18,19,24]. For example, in Lamb [19], the analytical calculation for the water level fluctuation as a result of total reflection was given, and in Parker [2] the superposition of the incident damped progressive wave with the reflected damped progressive wave as a result of total reflection was formulated, i.e., that the amplitudes of the two waves are equal at the location of the reflector. In Proudman [27], the standing oscillations in rivers, gulfs, and in channels were described in more detail: The damping effect due to friction is derived for rectangular basins. In Van Rijn [18], the formulation of the damped standing wave with a total reflection at a closed end was considered in an analytical model neglecting partial reflections at abrupt bathymetric changes.

The purpose of this paper is the following:

- To derive an analytical model that can be easily used to estimate the reflection and transmission coefficients of long period regular waves at abrupt bathymetric changes and thus increase the understanding of partial reflections;
- To establish a hydrodynamic numerical (HN) model capable of representing the reflection and transmission behavior of long waves (wavelengths of several hundreds of kilometers) while neglecting and reducing other dissipative effects.

An overview of the effect of a partial reflection on the surface elevations, the wave heights, and the velocities due to an abrupt bathymetric change is shown in Figure 1, in which the surface elevation and velocities of a tidal wave at different locations in a longitudinal section (A): downstream, B: upstream of the bathymetric change) is visible. The overall signal (blue) is the result of a linear superposition of the incident (black) and reflected (red) signal. The transmitted signal (violet) is located upstream of the abrupt bathymetric change (B). Flow velocities are superimposed by the incident, the reflected velocities from waves, and run-off from discharge. In Figure 1 the flow velocities of a propagating shallow water wave are shown, and they result from the time derivative of the surface elevation hydrograph. As a result of the reflected wave moving in the opposite

direction, the slack water points (green marker) are shifted. The lower graph shows the amplitude variation of the comprehensive tidal wave over the location. The amplitude variation of a partially standing wave can be seen.

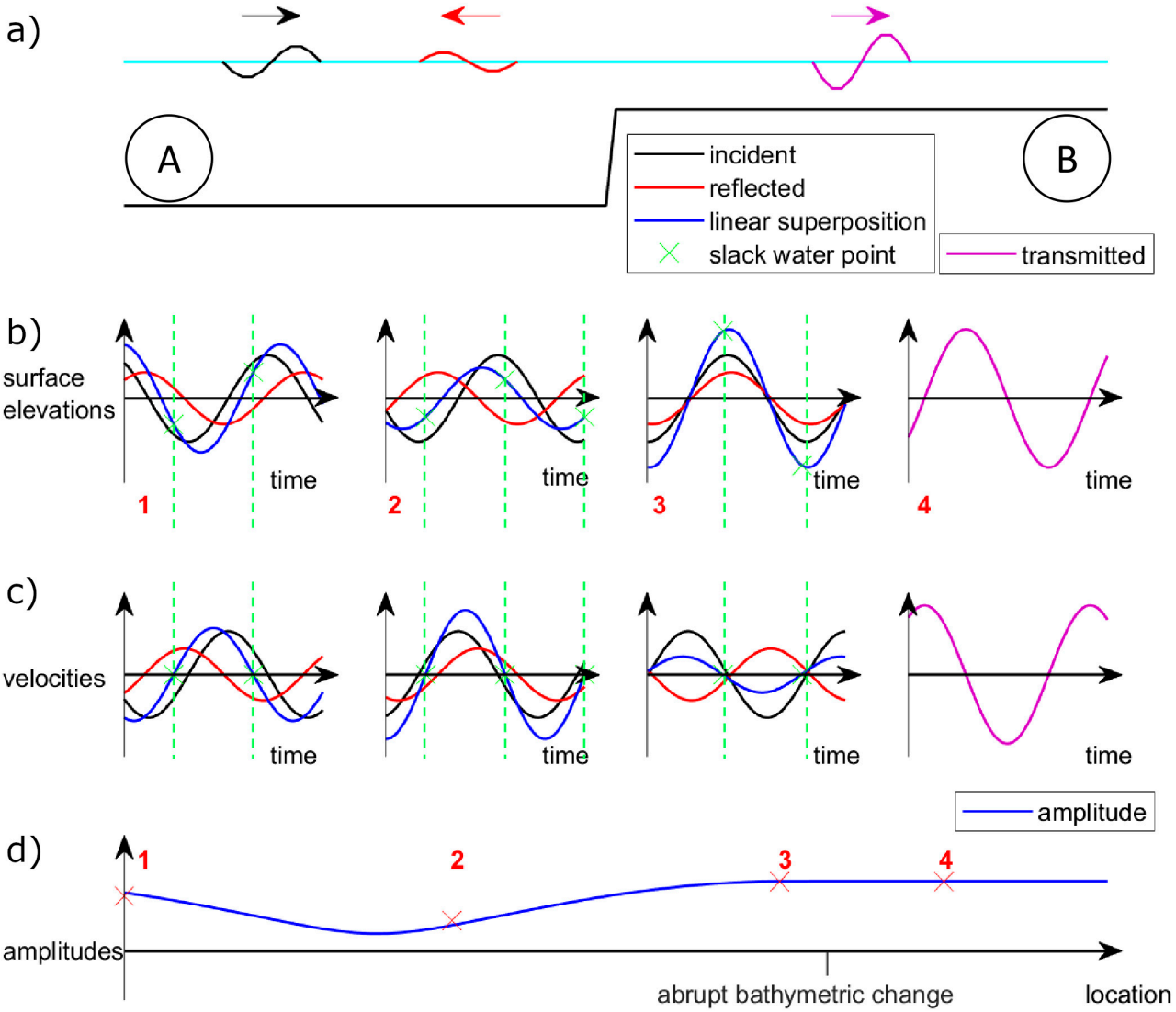


**Figure 1.** Simplified representation of the reflection and transmission of a tidal wave at an abrupt bathymetric change. In (**a**) the incident, reflected, and transmitted waves at an abrupt bathymetric change are shown with the corresponding surface elevations (**b**) and flow velocities (**c**) at three different locations downstream in the abrupt bathymetric change (area A) and one location upstream in the abrupt bathymetric change (area B). In (**d**) the amplitude of the overall signal (partial standing wave) is shown.

## 2. Materials and Methods

### *2.1. Theoretical Model for the Reflection of Linear Regular Waves at Bathymetric Changes*

The following investigation applies to tidal waves that are assumed to be periodic waves, i.e., waves composed of regular wave components with constant amplitude and frequency.

In the schematized model (Figure 1), no further reflections and re-reflections were initially considered. The theoretical model serves as a basis for the investigation of the reflection behavior and for the determination of the partial reflection at abrupt bathymetric changes. The model also neglects other influences on the tidal wave (e.g., headwater

discharge, islands, structures) in order to avoid having the amplitude and shape of the tidal wave along an estuary deviate from the theoretical model.

### *2.2. Energy-Based Approach*

An approach to calculate the partial reflection at bathymetric changes for long period waves was developed by Lamb [19] (see also Dean and Dalrymple [20]). The incident wave, which propagates in a positive x-direction (Figure 2) with the wave height $H_i$, encounters an abrupt bathymetric change. One part of the wave energy reflects, and the other part of the wave energy is transmitted. Energy dissipation is not taken into account. The calculation of the reflected and transmitted wave heights is based on the considerations that (i) any finite water level change over an infinitely small distance would give rise to infinite accelerations of the fluid particles, so that the water levels on each side of the step should be the same (long wave equations of motion) and (ii) the mass flow rates from regions located upstream and downstream of an abrupt bathymetric change are equal to another (continuity consideration). For the exact derivation, we refer to Lamb [19] or Dean and Dalrymple [20].

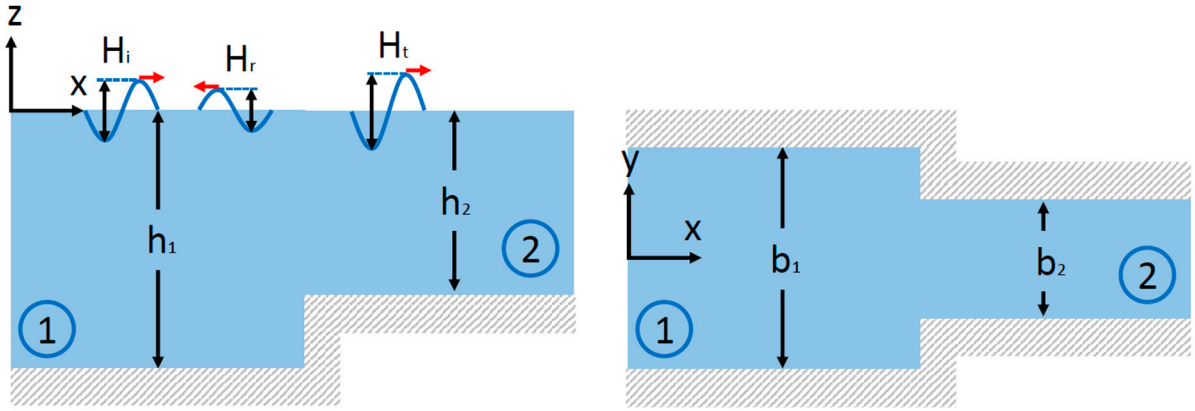


**Figure 2.** Cross-sectional and top view of an abrupt cross-sectional change. The wave heights $H_i$, $H_r$, and $H_t$ indicate the incident, reflected, and transmitted wave heights, respectively. The red arrows show the wave propagation direction. The numbers 1 and 2 indicate different locations with respective widths $b$ and depths $h$.

In the following, the reflection and the transmission of long waves are calculated using an energy-based approach. The waveform downstream (1) and upstream (2) (Figure 2) of the abrupt bathymetric change is calculated as follows:

$$\eta_1 = \eta_i + \eta_r = \frac{H_i}{2} \cdot cos(k_1 x - \sigma t) + \frac{H_r}{2} \cdot cos(k_1 x + \sigma t + \varphi_r), \quad (1)$$

$$\eta_2 = \eta_t = \frac{H_t}{2} \cdot cos(k_2 x - \sigma t + \varphi_t) \quad (2)$$

where $\eta$ describes the water level fluctuation, $k$ the wave number, $x$ the position, $\sigma$ the angular frequency, $t$ the time, and $\varphi$ the phase position. The indices $i$, $r$, and $t$ indicate the incident, reflected, and transmitted components, respectively. The change in depth results in a different wave number. The different phase angles include possible phase differences.

From the assumption of the linear superposition of incident and reflected waves, it follows that

$$\eta_i + \eta_r = \eta_t, \quad (3)$$

After additionally defining the reflection coefficient via $C_r = H_r / H_i$ and the transmission coefficient via $C_t = H_t / H_i$, the following condition applies:

$$1 + C_r = C_t \quad (4)$$

The wave energy of the incident waves ($E_i$) must correspond to the total wave energy of the reflected ($E_r$) and transmitted energies ($E_t$):

$$E_i = E_r + E_t \tag{5}$$

Therefore, Equation (5) gets the following:

$$\frac{\rho \cdot g \cdot H_i^2}{8} \cdot T \cdot b_i \cdot \sqrt{g \cdot h_i} = \frac{\rho \cdot g \cdot H_r^2}{8} \cdot T \cdot b_r \cdot \sqrt{g \cdot h_r} + \frac{\rho \cdot g \cdot H_t^2}{8} \cdot T \cdot b_t \cdot \sqrt{g \cdot h_t}, \tag{6}$$

where $\rho$ is the density of water, $g$ is the acceleration due to gravity, $b$ is the width, $H$ is the wave height (with the indices $i$, $r$, $t$ corresponding to the incident, reflected, and transmitted, respectively), $T$ is the wave period, and $h$ is the water depth. The water depths are in the corresponding areas downstream of the abrupt bathymetric change (1) and upstream of the abrupt bathymetric change (2), and thus the following applies:

$$H_i^2 \cdot b_1 \cdot \sqrt{h_1} = H_r^2 \cdot b_1 \cdot \sqrt{h_1} + H_t^2 \cdot b_2 \cdot \sqrt{h_2}, \tag{7}$$

and

$$\left(1 - C_r^2\right) \cdot b_1 \cdot \sqrt{h_1} = C_t^2 \cdot b_2 \cdot \sqrt{h_2} \tag{8}$$

Inserting Equation (4) into Equation (8) leads to

$$\left(1 - C_r^2\right) \cdot b_1 \cdot \sqrt{h_1} = (1 + C_r)^2 \cdot b_2 \cdot \sqrt{h_2} \tag{9}$$

Multiplying and reshaping results in the following:

$$C_r^2 \cdot \left(\frac{\sqrt{h_2} \cdot b_2}{\sqrt{h_1} \cdot b_1} + 1\right) + 2C_r \cdot \frac{\sqrt{h_2} \cdot b_2}{\sqrt{h_1} \cdot b_1} + \left(\frac{\sqrt{h_2} \cdot b_2}{\sqrt{h_1} \cdot b_1} - 1\right) = 0 \tag{10}$$

The solution of the quadratic equation leads to

$$C_{r-1,2} = -\frac{\sqrt{h_2} \cdot b_2 / \left(\sqrt{h_1} \cdot b_1\right)}{\sqrt{h_2} \cdot b_2 / \left(\sqrt{h_1} \cdot b_1\right) + 1} \pm \sqrt{\frac{h_2 \cdot b_2^2 / \left(h_1 \cdot b_1^2\right)}{\left(\sqrt{h_2} \cdot b_2 / \left(\sqrt{h_1} \cdot b_1\right) + 1\right)^2} - \frac{\sqrt{h_2} \cdot b_2 / \left(\sqrt{h_1} \cdot b_1\right) - 1}{\sqrt{h_2} \cdot b_2 / \left(\sqrt{h_1} \cdot b_1\right) + 1}} \tag{11}$$

Transforming and resolving leads to the reflection coefficient:

$$C_{r-1,2} = \pm \frac{1 - (b_2/b_1) \cdot \left(\sqrt{h_2}/\sqrt{h_1}\right)}{1 + (b_2/b_1) \cdot \left(\sqrt{h_2}/\sqrt{h_1}\right)} \tag{12}$$

The positive sign in the reflection coefficient is seen to be physically useful. With ratios $h_2 > h_1$ or $b_2 > b_1$, negative signs in the reflection coefficient are generated, which indicate a phase jump of 180°. Inserting Equation (12) into Equation (8) leads to the transmission coefficient:

$$C_t^2 = \left(1 - \left(\frac{1 - \frac{b_2}{b_1} \cdot \frac{\sqrt{h_2}}{\sqrt{h_1}}}{1 + \frac{b_2}{b_1} \cdot \frac{\sqrt{h_2}}{\sqrt{h_1}}}\right)^2\right) \frac{\sqrt{h_1} \cdot b_1}{\sqrt{h_2} \cdot b_2} \tag{13}$$

The reformulation results in the following:

$$C_t = \frac{2}{1 + \frac{b_2}{b_1} \cdot \frac{\sqrt{h_2}}{\sqrt{h_1}}} \tag{14}$$

These solutions agree with the analytical solutions in Lamb [19] and Dean and Dalrymple [20]. With these results, diagrams for the assessment of wave reflection and wave

transmission at different widths and depths are derived. Figures 3 and 4 visualize the reflection and transmission coefficients for different depth ratios and a constant width ratio. The gray shaded area indicates a phase jump of 180°. If $h_1 = h_2$, the reflection coefficient is 0, and the transmission coefficient is 1 because no reflection occurs. If the ratio of $h_1/h_2$ increases, the reflection coefficient increases and finally approaches 1 (i.e., total reflection), and the transmission coefficient approaches 2 (i.e., superposition of the incident and reflected wave). If the ratio of $h_2/h_1$ increases, the reflection coefficient increases with a phase jump of 180° and finally approaches 1 (total reflection), and the transmission coefficient approaches asymptotically 0 (wave energy remains in area 2, i.e., upstream of the abrupt bathymetric change).

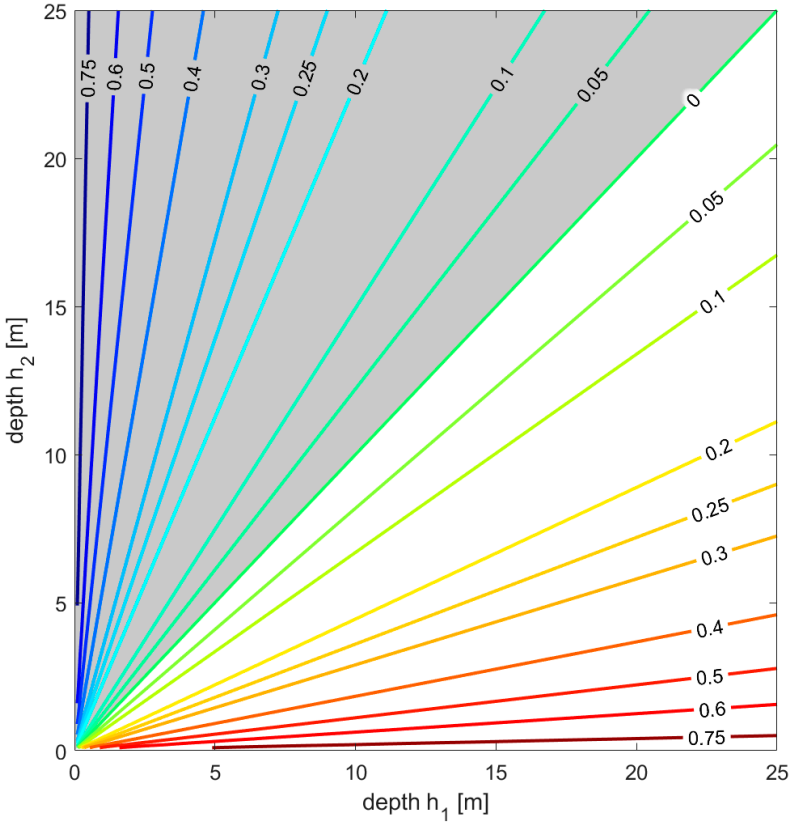


**Figure 3.** Visualization of the reflection coefficient at abrupt bathymetric changes for different depths and constant widths upstream and downstream of the bathymetric change. The gray shaded area indicates reflection with a phase jump of 180°.

### *2.3. Hydrodynamic Numerical Simulations*

To solve the equations of continuity and momentum including nonlinear terms and reflection, numerical models can be used, using either a 1D cross-section-averaged approach, a 2DH depth-averaged approach, or a 3D approach. To investigate and evaluate the fundamental influence of different conditions on the reflection behavior, a basis model (simplified channel) was used. Submodels were derived from the basic model into which the different conditions were integrated. These models were used to simulate single or multiple waves of a tidal constituent ($M_2$). Reflection coefficients were determined from the simulation results. Furthermore, a harmonic analysis method (Fast Fourier Transform, FFT) was applied to the simulation results of several waves.

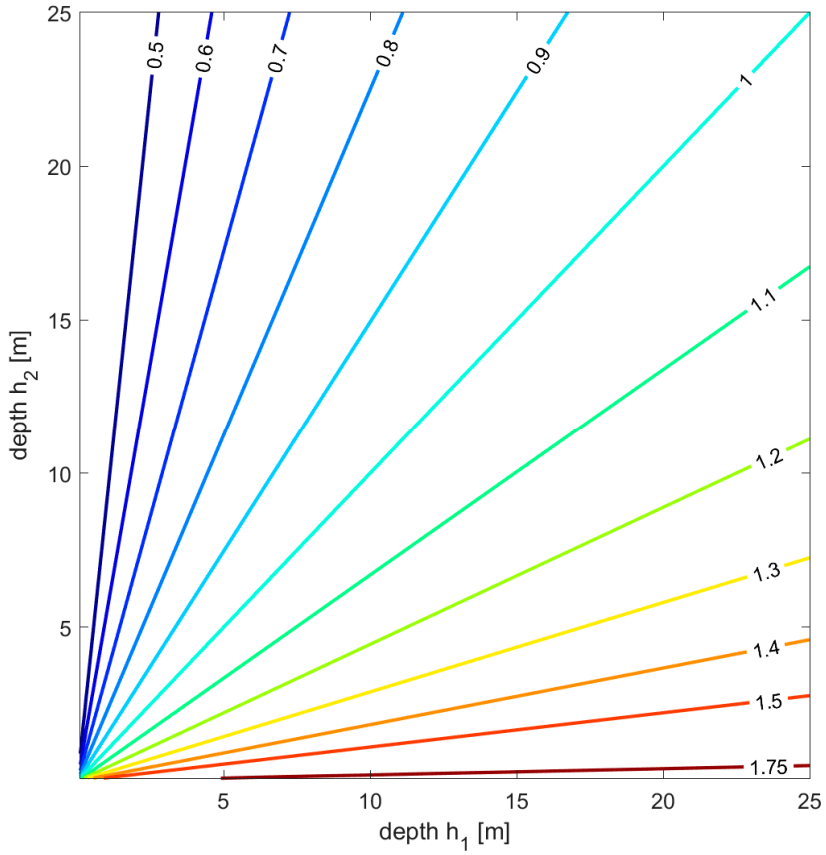


**Figure 4.** Visualization of the transmission coefficient at abrupt bathymetric changes for different depths and constant widths upstream and downstream of the bathymetric change.

The preprocessing was done with Kalypso1D2D. For the numerical modelling, TELEMAC2D was used, which solves the shallow water wave equations in two dimensions. The postprocessing was performed using TecPlot and MATLAB. The inflow of a sinusoidal wave signal induced by the $M_2$ tide with an amplitude of 0.1 m over a water level boundary condition was simulated. Since the deformation of the tidal wave in shallow water (meaning that the wave propagation speed of the wave crest is higher than that of the wave trough) depends on the ratio between the tidal amplitude and depth (see e.g., [23]), the amplitude was chosen to be relatively low (0.1 m) to reduce the deformation effect. Table 1 provides an overview of the model dimensions and settings used. The spatial model extent is necessary in order to identify the incident, transmitted, and reflected long-period waves directly in the model. The friction coefficients and the turbulence parameter (viscosity coefficient) were selected in the given (very low) range with the aim to keep the dissipative effects in the model extent as low as possible in order to simulate only the reflection and transmission processes.

An example of the result of the simulation with the hydrodynamic numerical (HN) model is shown in Figure 5. In the upper row (from middle to right), the velocities along the longitudinal axis (x) and the node heights are shown. From the mesh geometry (Figure 5b), the abrupt bathymetric change with a length of 13.7 km (indicated with an orange dotted line and labelled with the number 5) can be seen. The length of the abrupt bathymetric change was approximated to the bathymetry of the river Elbe. In Figure 5 c, the simulated free water surface elevation at two simulation time steps is shown. The simulated free water surface elevation is shown over time at different positions in the channel in the diagram (d) in Figure 5. At x = 0 km, there is the model boundary (label 1) where the wave (black) gets inserted over a water level boundary condition. At x = 700 km (red), the incident (green background, see also label 2) and the reflected (yellow background, see also

label 3) signals can be identified. At x = 1200 km (green, label 4), the transmitted signal is seen.

**Table 1.** Overview of model extent and simulation settings.

| | **Basic Model: Simulation of Single Wave** | **Submodel: Simulation of Multiple Waves** |
|---|---|---|
| Model extent [1] | x = 2000 km; y = 3 km; z = varying | $x^2$ = 20,000 km; y = 3 km; $z_1 = -17$ m; $z_2 = -6$ m |
| Grid resolution | $\Delta x$ = 600 m; $\Delta y$ = 150 m | $\Delta x$ = 600 m; $\Delta y$ = 150 m |
| Boundary conditions | 1 water level boundary [3]<br>$M_2$ signal (1 wave)<br>Amplitude = 0.1 m<br>Initial condition = elevation of 0 m | 1 water level boundary<br>$M_2$ signal (15 waves)<br>Amplitude = 0.01 m<br>Initial condition = elevation of 0 m |
| Time resolution | Simulation duration [1] $\approx$ 46.3 h<br>Time step = 1 s<br>Printout period = 5 min | Simulation duration $\approx$ 17.85 days<br>Time step = 1 s<br>Printout period = 15 min |
| | **Physical processes** | |
| Friction | No bottom or sidewall friction | No bottom or sidewall friction |
| Turbulence model | Constant viscosity [4] | Constant viscosity |
| Meteorological phenomena | No consideration of meteorological phenomena, e.g., wind, atmospheric pressure, rain | No consideration of meteorological phenomena |

[1] The model extent and the simulation duration were chosen to separate the incident and reflected tidal waves (both for one wave and multiple waves) while avoiding re-reflection at the boundaries. [2] The dimension of x = 20,000 km is valid for the simulation of the partial reflection. To include a total reflection of the tidal waves, the model is 10,138 km long. [3] Since the model is numerically underdetermined, the Thompson method was used for the boundary condition [28]. [4] The constant viscosity coefficient represents the molecular and turbulent viscosity and corresponds to the molecular viscosity of water ($10^{-6}$ $m^2/s$). Therefore, the dissipation has a negligible effect on the tidal waves.

By the separation of the incident and the reflected signals (with corresponding amplitudes), the reflection coefficient from the reflection of the tidal wave at abrupt bathymetric changes can be calculated.

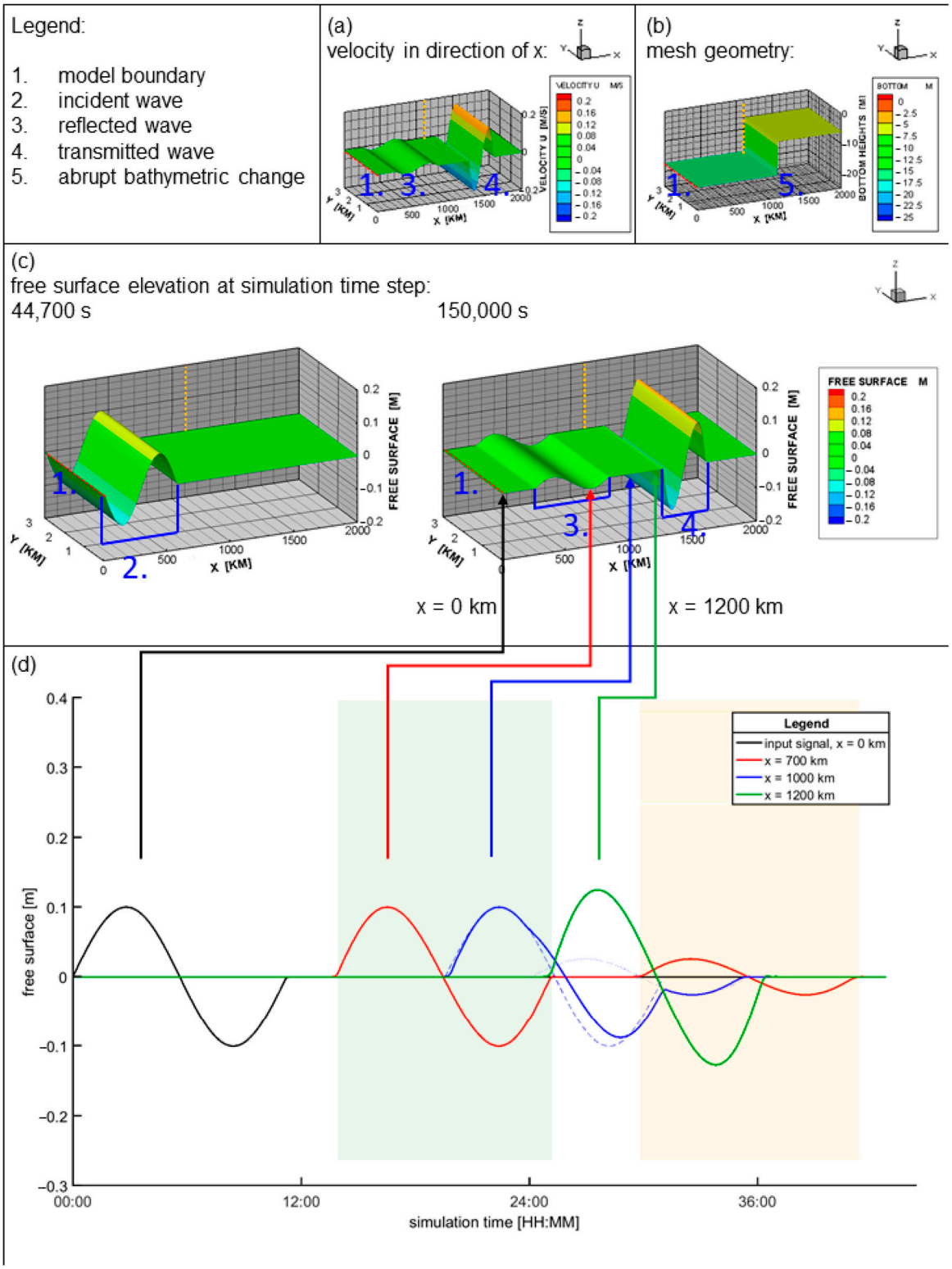


**Figure 5.** Local and temporal representation of simulation results from the hydrodynamic numerical (HN) model including all harmonics: (**a**) velocity in x-direction; (**b**) mesh geometry with the abrupt bathymetric change at around x = 1100 km; (**c**) free surface elevation at the simulation time steps $t$ = 44,700 s and 150,000 s; and (**d**) temporal representation of the simulated water level elevation at different locations, where the green and yellow backgrounds indicate the incident and reflected waves at x = 700 km (red line), respectively; the dashed blue indicates the incident wave and the dotted blue line the reflected wave at x = 1000 km.

## 3. Results

In order to get a general explanation of the reflection behavior of tides at abrupt bathymetric changes observed in estuaries, attention initially is given to the reflection behavior of the principal lunar semi-diurnal tide constituent, usually denoted by $M_2$. The $M_2$ constituent is a regular harmonic motion with a period of $T \cong 12.42$ h ($T \cong 12$ h 25 min) and with locally varying amplitude.

From the local representation (Figure 5c) of the simulated data from the hydrodynamic numerical (HN) model, a shorter wavelength in the shallower area than in the deeper area can be seen. This observation generally agrees with the calculation of the wavelength $L$ using the linear wave theory (Airy) for shallow water waves ($L = T \cdot \sqrt{g \cdot h}$, with $T$ as wave period, $g$ as gravity acceleration constant, and $h$ the water depth).

The amplitude of the reflected signal is lower than the amplitude of the incident signal. From the temporal representation, it is seen that the period remains constant. This also agrees with the physical properties of wave motion. The amplitude of the incident wave signal is the same (no damping) at both locations of x = 0 km and x = 700 km. Focusing on the black line (x = 0 km), it becomes obvious that the reflected signal is not generated by the given boundary condition but is only generated by the reflection at the bathymetric change. On the basis of the partially reflected signal, after a determination of the amplitudes, a reflection coefficient of

$$C_r = \frac{a_r}{a_i} = \frac{0.0252m}{0.1m} = 25.2\% \quad (15)$$

for an abrupt bathymetric change with the abovementioned locations and channel dimensions can be calculated.

The free surface elevation over time in Figure 5 (x = 1000 km, blue) shows the deformation of the composed tidal wave because of reflection (at a simulation time of approx. 24 h). The blue dashed line indicates the incident signal and the dotted line the reflected signal. By linear superposition of the two elevation values for the incident and reflected waves, the resulting free water surface elevation is calculated. The transmitted signal at x = 1200 km (green) shows an expected increase in amplitude because of shoaling after a cross-sectional constriction.

To compare the HN-simulation results with those of the energy-based approach developed in Section 2.2., submodels with different mesh heights were created and simulated with the HN model. The results from the HN simulations are compared with the energy-based approach under the abovementioned assumptions for a variety of water depths conditions. The parameter combinations as well as the resulting simulated reflection coefficients are given in Table 2.

**Table 2.** Comparison of calculated and simulated reflection coefficients for different depths.

| Water Depth $h_1$ (m) | Water Depth $h_2$ (m) | Reflection Coefficient (Analytical) | Reflection Coefficient (Simulation) | Relative Deviation |
|---|---|---|---|---|
| 17 | 17 | 0% | 0% [1] | 0% |
| 24.3 | 15 | 12% | 12% | 0% |
| 17 | 10 | 13.2% | 13.3% | 0.8% |
| 17 | 6 | 25.5% | 25.2% | 1.2% |
| 8 | 2 | 33.3% | 32.6% | 2.1% |
| 17 | 2 | 48.9% | 48.3% | 1.2% |
| 8 | 0.5 | 60% | 58.1% | 3.2% |
| 20 | 0.5 | 72.7% | 72.1% | 0.8% |
| 17 | 0 | 100% | 100% [2] | 0% |

[1] The simulation was performed with a HN model without depth change. [2] The simulation was carried out with a total reflector (run-up of the wave against the edge of the mesh).

The values of the analytical model agree well with those of the simulated model (relative deviation less than 5%). The calculated transmission coefficients are given in

Table 3. Comparing the results of the analytical solution and the simulation results, a maximum relative deviation of around 4% can be seen. In general, it can be stated that the hydrodynamic numerical simulations match the analytical solutions for a wide variety of different bottom steps.

**Table 3.** Comparison of calculated and simulated transmission coefficients for different depths.

| Water Depth $h_1$ (m) | Water Depth $h_2$ (m) | Transmission Coefficient (Analytical) | Transmission Coefficient (Simulation) | Relative Deviation |
|---|---|---|---|---|
| 17 | 17 | 100% | 100% [1] | 0% |
| 24.3 | 15 | 112% | 111.7% | 0.3% |
| 17 | 10 | 113.3% | 112.9% | 0.4% |
| 17 | 6 | 125.5% | 124.4% | 0.9% |
| 8 | 2 | 133.3% | 130% | 2.5% |
| 17 | 2 | 149% | 146.2% | 1.9% |
| 8 | 0.5 | 160% | 153.8% | 3.9% |
| 20 | 0.5 | 172.7% | 173.6% | 0.5% |
| 17 | 0 | 0% | 0% [2] | 0% |

[1] The simulation was performed with a HN model without depth change. [2] The simulation was carried out with a total reflector (run-up of the wave against the edge of the mesh).

The differences between the analytical solution and the numerical solution are a result of the approximation of the abrupt bathymetrical change in the HN model, where initially a slope and not an abrupt depth step was applied for numerical approximation. The influence of the mesh density on the results of the HN model was determined in a mesh convergence study. Here, changes in the reflection coefficients in the third significant digit were found. When the length of the abrupt bathymetric change (bottom step) was reduced, it was apparent that the shorter the bathymetric change became (i.e., the more "abrupt"), the closer the reflection coefficient from the HN simulation approached the analytical solution, showing a clear convergence toward the analytical energy-based approach. For clarification, the convergence tests were carried out for a bottom step with $h_1$ = 17 m and $h_2$ = 6 m as example.

Additionally to the analysis of a simple bottom step, a combination of a bottom step and a width reduction (increase) was also analyzed. Methodologically, both methods mentioned above were applied. The results are given in Tables 4 and 5 in analogy to those in Tables 2 and 3. The reflection coefficients (in Table 4) and the transmission coefficients (in Table 5) from the analytical model and the HN simulations for a cross sectional constriction from the water depth 17 m to 6 m and different width ratios are compiled. Comparing both the reflection and transmission coefficients from the analytical and HN models, the relative deviation for the reflection and transmission coefficients is less than 1.0%.

**Table 4.** Comparison of calculated and simulated coefficients for a depth ratio 17/6 and different width ratios.

| Width $b_1$ (m) | Width $b_2$ (m) | Reflection Coefficient (Analytical) | Reflection Coefficient (Simulation) | Relative Deviation |
|---|---|---|---|---|
| 3000 | 3000 | 25.4% | 25.2% | 0.8% |
| 550 | 470 | 32.6% | 32.4% | 0.6% |
| 5000 | 3000 | 47.3% | 47.2% | 0.2% |
| 1000 | 500 | 54.2% | 53.9% | 0.6% |
| 3000 | 1000 | 66.9% | 66.7% | 0.3% |
| 10,000 | 3000 | 69.7% | 69.5% | 0.3% |
| 3000 | 500 | 82% | 81.8% | 0.2% |

**Table 5.** Comparison of calculated and simulated transmission coefficients for a depth ratio 17/6 and different width ratios.

| Width $b_1$ (m) | Width $b_2$ (m) | Transmission Coefficient (Analytical) | Transmission Coefficient (Simulation) | Relative Deviation |
|---|---|---|---|---|
| 3000 | 3000 | 125.4% | 124.4% | 0.8% |
| 550 | 470 | 132.6% | 131.5% | 0.8% |
| 5000 | 3000 | 147.3% | 146.1% | 0.8% |
| 1000 | 500 | 154.2% | 152.7% | 1.0% |
| 3000 | 1000 | 166.9% | 165.4% | 0.9% |
| 10,000 | 3000 | 169.7% | 168.6% | 0.6% |
| 3000 | 500 | 182.0% | 180.1% | 1.0% |

To describe the impact of a wave propagating against a widening of the cross section, a tidal wave was implemented at the upper boundary of the HN model, and the reflection coefficient(s) was evaluated. From the simulation of a wave moving against a widening of the cross section, a partial reflection (same reflection coefficient as a similar cross-sectional constriction) with a phase shift of 180° ($\pi$) can be seen. The transmitted signal is reduced. The reflection and transmission coefficients of the HN simulation test almost perfectly agree with the analytical solution.

The tide does not only consist of a single tidal wave but of an (almost) infinite number of waves (tidal constituents). In order to analyze the amplification of higher harmonic tidal constituents, an HN submodel was created, into which several regular waves were inserted at the boundary. A wave with the period of the $M_2$ tide was inserted into the model at the left water level boundary. In the model, the waves are partially as well as totally reflected at different reflectors (see Figure 5b) with a partial reflector at x = 10,100 km, and an additionally added total reflector at x = 10,138 km at the right boundary. The simulation results were analyzed by harmonic analysis (FFT) in order to determine the behavior of the individual constituents while propagating in an estuary. The analysis was performed for signals at different locations in the model estuary and plotted in a longitudinal section (Figure 6).

In Figure 6, the results of the harmonic analysis of the simulations data are shown. In the area between the partial and total reflectors (from about 10,100 km to 10,138 km, see also Figure 6b), the $M_2$ signal reaches an amplification above 2 by the partially reflected (and then, again, totally reflected and re-reflected) signal, which is caused by the superposition of the partial and total reflection. In Figure 6a, the generation of the $M_4$ tidal constituent can be seen: In addition to the inserted $M_2$ constituent, a $M_4$ tidal constituent was generated, originating from shallow water effects and amplified because of the interaction with the reflection points. A clear standing wave was analyzed in the model reach, and an additional amplification of the $M_4$ constituent was observed in the area between the total reflector and the partial reflector. The proportion of the $M_4$ component to the inserted $M_2$ component reaches maximum of 7.81%. Focusing on the area between 10,000 km to 10,138 km in Figure 6b, the additional generation of further higher harmonic components (here $M_6$ and $M_8$) can be seen. However, the proportion of the $M_6$ and $M_8$ components reaches only 0.82% ($M_6$) and 0.17% ($M_8$) at maximum, respectively, of the inserted $M_2$ component, due to the neglected friction effects and the reduction of the deformation of the tidal wave by a low amplitude–depth ratio. If the amplitude of the $M_2$ component at the model boundary is increased by a factor of 10, the respective proportions at the maximum are 45% ($M_4$), 27.9% ($M_6$) and 20.1% ($M_8$).

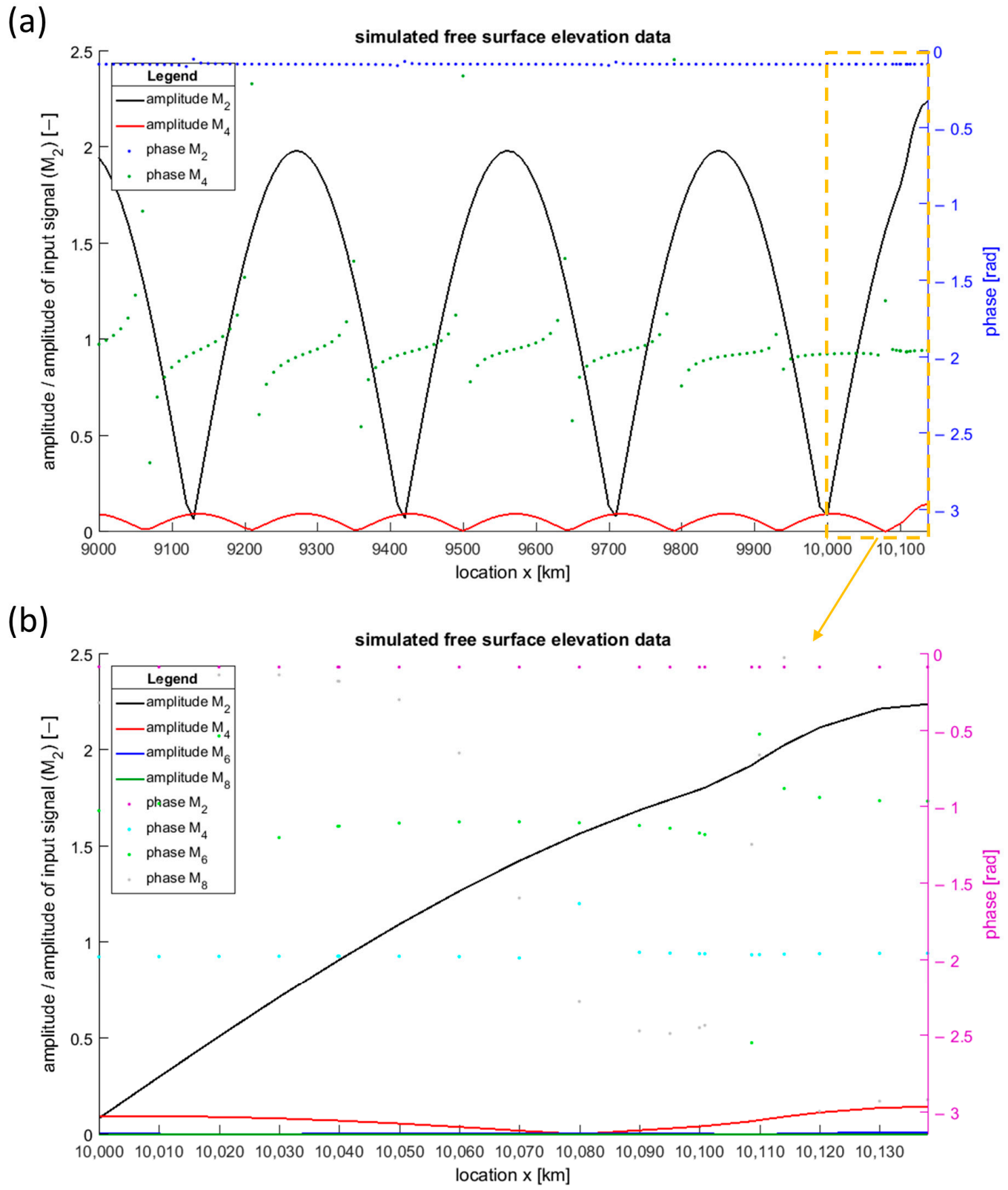


**Figure 6.** Visualization of the harmonic analysis results of the simulations data along the length sections from a model with a bathymetric change (at x = 10,100 km), constant model widths and a total reflector (x = 10,138 km): (**a**) the harmonic analysis results of the simulation data from x = 9000 km to 10,138 km for the $M_2$ and $M_4$ constituents; (**b**) the harmonic analysis results of the simulation data from x = 10,000 km to 10,139 km with additional representation of $M_6$ and $M_8$ constituents.

Maximum amplification as a result of partial and total reflection is achieved at a distance from the partial to total reflector of one quarter of the wavelength in the area upstream of the abrupt bathymetric change (not shown here). The amplification in the area between two reflectors can be imagined as a series converging towards a limit value.

The analytical model is not able to represent the generation of higher harmonics due to shallow water effects, since these effects were not considered in the equations.

Due to the superposition of the partial and total reflection, there is no full standing wave (clapotis) in the system, where the amplification is zero in some places. At the extreme values of the amplifications of the $M_2$ tide, the maxima of the amplifications of the higher harmonic component $M_4$ tide appear.

If a friction component (roughness coefficient of $10^{-5}$ m, Nikuradse law) is additionally integrated in the HN model (Figure 7), the occurrence of further higher harmonic components (especially $M_6$, partly $M_8$ and $M_{10}$–$M_{10}$ not shown in Figure 7) becomes apparent. The amount of friction in the HN model is relatively low to allow the tidal wave to proceed. The observation of the generation of the $M_6$ due to friction effects generally agrees with the tidal prediction made in Parker [2]. In Parker's explanation on the symmetric and asymmetric effects of bottom friction, the asymmetric effect on the tidal wave is due to the higher effects of friction in shallow water than in deep water (wave trough being more slowed down than the wave crest), which leads to the generation of $M_4$. The symmetric effect results from the energy loss because of friction, which is proportional to the square of the current speed (more energy loss during maximum flood, less energy loss during maximum ebb), which leads to the generation of $M_6$ [2].

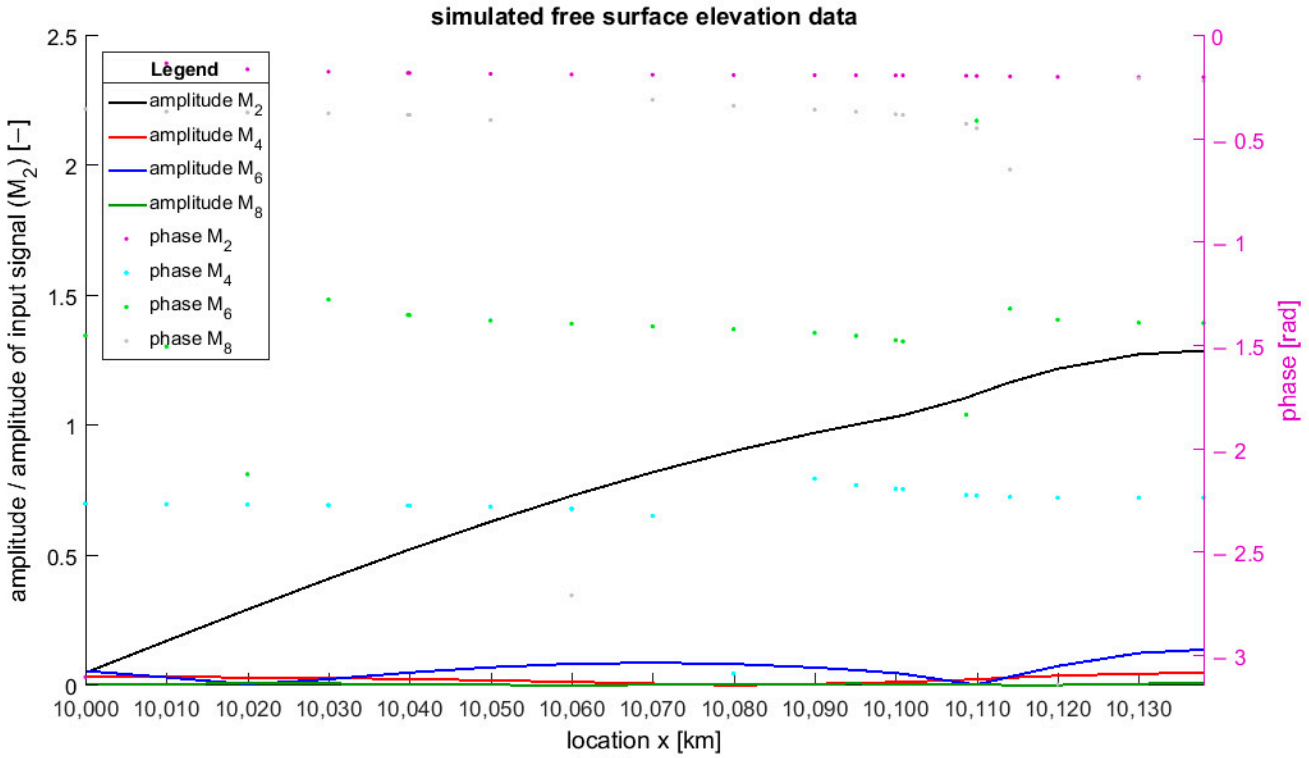


**Figure 7.** Visualization of the harmonic analysis results ($M_2$, $M_4$, $M_6$, $M_8$) of the simulation data along the length sections section from x = 10,000 km to 10,139 km from a model with a bathymetric change (at x = 10,100 km), constant model widths and a total reflector (x = 10,138 km).

## 4. Discussion

Reflection and transmission coefficients at abrupt geometric changes were calculated using a simplified energy-based analytical model and a hydrodynamic numerical (HN)

model, to better understand the influence of geometric changes at which the tidal wave is reflected on hydrodynamics in estuaries. The comparison of results show a high agreement of the results of the different methods.

The analytical model leads to good estimates of the reflection and transmission coefficient compared to the HN models for long-period regular waves. Using the analytical model, it is possible to make statements about the change of the theoretical reflection and transmission coefficients when abrupt changes of cross sections occur. The effect of an abrupt change in width on the reflection and transmission coefficients is greater than the change in depth ratios to the same extent. The analytical model can theoretically be used for regular long-period waves regardless of period as long as the bathymetric change is abrupt compared to the incident wavelength. The larger the ratio of the length of the abrupt bathymetric change to the wavelength becomes, the larger the deviations of the analytical model from the solutions from the HN model are.

The HN simulations show a clear separation of the incident, reflected, and transmitted tidal waves as a result of the model extent and the simulation settings. The following statements are derived from the investigations carried out with the numerical model and the energy-based approach:

- Reflectors for tidal waves are abrupt cross-sectional changes in an estuary. The reflection behavior of the cross-sectional changes can be analyzed by HN models as well as with analytical models.
- With the energy-based analytical approach and in the HN model, identical results are obtained for cross-sectional changes with regard to the transmitted and reflected waves.
- A wave is not only partially reflected by an abrupt reduction in cross section but also by an abrupt expansion of the cross section. The degree of reflection is the same as that for a reflection at a cross-sectional reduction, but there is a phase shift of 180° ($\pi$).
- If an HN model is forced at its boundary by several waves of one tidal constituent ($M_2$), higher harmonic tidal constituents ($M_4$, $M_6$, $M_8$) are obtained and amplified as visualized in this paper. As written in [22,23] the generation of higher harmonics is a result of shallow water effects on the wave motion and reflection properties of an estuary.
- The tidal constituents are reflected at partial (cross-sectional changes) and total reflectors and amplified by shoaling, and as a result the shallow water tidal constituents generated from the $M_2$ are significantly amplified.

The model investigations show a realistic behavior and a high agreement in the results of the energy-based approach. These investigations are valid for the principal lunar semi-diurnal tide constituent, which is often found in estuaries as a dominant tide.

The oscillation system of a real estuary is more complex than that of a simple channel model. However, the investigations do provide an insight into the complex processes in an estuary: The tidal wave deforms as it enters the estuary due to numerous factors such as cross-sectional changes, roughness influences, meanders, and headwater, and it is partially and totally reflected by several reflectors. The main reflectors are total reflectors such as weirs and partial reflectors such as abrupt cross-sectional changes, harbor entrances, branches, etc. Upstream of a bathymetric change (partial reflector), the transmitted signal moves on to the total reflector, where the transmitted signal is totally reflected. The reflected wave moves in the opposite direction back toward the bathymetric change. At this bathymetric change, the reflected signal is again partially reflected (this time with a phase jump of 180°) and transmitted in the downstream direction. The transmitted part is superimposed on the incoming and reflected wave. This idea can be continued indefinitely and illustrates the complexity of the oscillation system, which is set in estuaries.

## 5. Conclusions

Since the existing approaches for calculating reflection coefficients for long waves, such as gauge methods, empirical methods, or analytical models, either do not sufficiently account for the partial reflections and re-reflections occurring at abrupt bathymetric changes

or lack the specification of reflection coefficients for tidal waves in estuaries, where damping of the tidal wave plays an important role, a simple-to-use analytical model based on wave energies was derived here for long period waves and compared with the results from a HN model.

With the comparatively simple energy-based analytical model, reflection and transmissions coefficients based on the width and depth conditions upstream and downstream of abrupt bathymetric changes were calculated. Since only the depth and width conditions at the bathymetric change are used, this approach is very easy to apply to certain conditions. Based on this approach, existing gauge methods or analytical estuarine models can be further developed in order to analyze the partial reflection of tidal waves in estuaries (e.g., at bathymetric changes as a result of dredging activities or estuarine mouth areas where the widths and depths change abruptly). In addition, the analytical model developed can be applied to understand the reflection processes that occur at abrupt bathymetric changes, and this allows for conclusions about the effects of both width and depth ratio changes. Further development of the approaches are required to include dissipation effects: In the simplified approach shown here, no damping factors (such as turbulence or friction effects) were taken into account.

The hydrodynamic numerical model solves the full (linearized) shallow water equations and can therefore be applied to assess nonlinear effects related to reflection and transmission at abrupt bathymetrical changes in estuaries. In order to be able to compare the derived analytical model with the numerical results, an approach was developed which allows for the direct identification of the incident, the transmitted, and the reflected signals. In this approach, dissipative effects were removed wherever possible in the numerical model. In addition, the model boundaries were selected in a way that they do not influence the separation area by reflection or re-reflection.

With the results shown here, the process understanding of partial and total reflections is increased. It becomes apparent where reflections and re-reflections of tidal waves occur in an estuary and to what extent reflections and transmission change the tidal wave system in an estuary. Future work will include damping effects of the tidal waves.

**Author Contributions:** Conceptualization, P.F. and V.S.; methodology, V.S.; software, V.S.; validation, S.S.V.H., T.S., E.N., P.F. and V.S.; formal analysis, V.S.; investigation, V.S.; writing—original draft preparation, V.S.; writing—review and editing, V.S., S.S.V.H., E.N., T.S. and P.F.; visualization, V.S.; supervision, E.N., T.S. and P.F.; project administration, E.N., T.S. and P.F.; funding acquisition, T.S. and P.F. All authors have read and agreed to the published version of the manuscript.

**Funding:** This research was funded by Federal Ministry of Education and Research (Germany), grant number 03KIS121.

**Institutional Review Board Statement:** Not applicable.

**Informed Consent Statement:** Not applicable.

**Acknowledgments:** The studies presented in this publication are part of the German Coastal Engineering Research Council (KFKI) project RefTide. We acknowledge support for the Open Access fees by Hamburg University of Technology (TUHH) in the funding program Open Access Publishing.

**Conflicts of Interest:** The authors declare no conflict of interest. The funders had no role in the design of the study; in the collection, analyses, or interpretation of data; in the writing of the manuscript, or in the decision to publish the results.

## References

1. Clark, R.H. *Elements of Tidal-Electric Engineering*; IEEE Press Wiley-Interscience; IEEE Xplore: Piscataway, NJ, USA, 2007. [CrossRef]
2. Parker, B.B. *Tidal Analysis and Prediction*; Center for Operational Oceanographic Products and Services: Silver Spring, MD, USA, 2007.
3. Díez-Minguito, M.; Azofra, A.B.; Ortega-Sánchez, M.; Rodríguez, M.A.L. Tidal Reflection. In *Encyclopedia of Estuaries*; Ken-nish, M.J., Ed.; Springer: Dordrecht, The Netherlands, 2016; pp. 704–706.
4. Goda, Y.; Suzuki, T. Estimation of incident and reflected waves in random wave experiments. In Proceedings of the 15th Confer-ence on Coastal Engineering, Honolulu, Hawaii, 11–17 July 1976.

5. Mansard, E.P.D.; Funke, E.R. The measurement of incident and reflected spectra using a least squares method. In Proceedings of the 17th Conference on Coastal Engineering, Sydney, Australia, 23–28 March 1980; ASCE: Reston, VA, USA, 1980; pp. 154–172.
6. Baldock, T.; Simmonds, D. Separation of incident and reflected waves over sloping bathymetry. *Coast. Eng.* **1999**, *38*, 167–176. [CrossRef]
7. Brossard, J.; Hémon, A.; Rivoalen, E. Improved analysis of regular gravity waves and coefficient of reflexion using one or two moving probes. *Coast. Eng.* **2000**, *39*, 193–212. [CrossRef]
8. Davidson, M.; Bird, P.; Huntley, D.; Bullock, G. Prediction of wave reflection from rock structures: An integration of field & laboratory data. *Int. Conf. Coastal. Eng.* **1996**, *1*, 2077–2086.
9. Renouard, D.P.; Santos, F.; Temperville, A.M. Experimental study of the generation, damping, and reflexion of a solitary wave. *Dyn. Atmos. Ocean.* **1985**, *9*, 341–358. [CrossRef]
10. Sutherland, J.; O'Donoghue, T. Wave Phase Shift at Coastal Structures. *J. Waterw. Port Coast. Ocean Eng.* **1998**, *124*, 90–98. [CrossRef]
11. Wiegel, R.L. Water wave equivalent of mach-reflection. In Proceedings of the 9th Conference on Coastal Engineering; ASCE, Ed.; American Society of Civil Engineers: New York, NY, USA, 1964; pp. 82–102.
12. Hunt, J.N. Tidal Oscillations in Estuaries. *Geophys. J. Int.* **1964**, *8*, 440–455. [CrossRef]
13. Dronkers, J.J. The schematization for tidal computations in case of variable bottom shape. *Int. Conf. Coastal. Eng.* **1972**, *1*, 2379–2396. [CrossRef]
14. Prandle, D.; Rahman, M. Tidal Response in Estuaries. *J. Phys. Oceanogr.* **1980**, *10*, 1552–1573. [CrossRef]
15. Friedrichs, C.T.; Aubrey, D.G. Tidal propagation in strongly convergent channels. *J. Geophys. Res.* **1994**, *99*, 3321. [CrossRef]
16. Lanzoni, S.; Seminara, G. On tide propagation in convergent estuaries. *J. Geophys. Res.* **1998**, *103*, 30793–30812. [CrossRef]
17. Savenije, H.; Toffolon, M.; Haas, J.; Veling, E. Analytical description of tidal dynamics in convergent estuaries. *J. Geophys. Res.* **2008**, *113*, C10025. [CrossRef]
18. Van Rijn, L.C. Analytical and numerical analysis of tides and salinities in estuaries: Part I: Tidal wave propagation in con-vergent estuaries. *Ocean Dyn.* **2011**, *61*, 1719–1741. [CrossRef]
19. Lamb, H. *Hydrodynamics*, 6th ed.; University Press: Cambridge, UK, 1932.
20. Dean, R.G.; Dalrymple, R.A. *Water Wave Mechanics for Engineers and Scientists*; World Scientific Publishing Company: Singapore, 1991.
21. Lin, P. A numerical study of solitary wave interaction with rectangular obstacles. *Coast. Eng.* **2004**, *51*, 35–51. [CrossRef]
22. Le Cann, B. Barotropic tidal dynamics of the Bay of Biscay shelf: Observations, numerical modelling and physical interpre-tation. *Cont. Shelf Res.* **1990**, *10*, 723–758. [CrossRef]
23. Pingree, R.D.; Griffiths, D.K.; Maddock, L. Quarter diurnal shelf resonances and tidal bed stress in the English Channel. *Cont. Shelf Res.* **1984**, *3*, 267–289. [CrossRef]
24. Díez-Minguito, M.; Baquerizo, A.; Ortega-Sánchez, M.; Ruiz, I.; Losada, M.A. Tidal Wave Reflection from the Closure Dam in the Guadalquivir Estuary (SW Spain). *Int. Conf. Coastal. Eng.* **2012**, *1*, 58–66. [CrossRef]
25. Baquerizo, A. Reflexión del Oleaje en Playas: Métodos de Evaluación y de Predicción. Ph.D. Thesis, Universidad de Cantabria, Santander, Spain, 1995.
26. Díez-Minguito, M.; Baquerizo, A.; Ortega-Sánchez, M.; Navarro, G.; Losada, M.A. Tide transformation in the Guadalquivir estuary (SW Spain) and process-based zonation. *J. Geophys. Res.* **2012**, 117. [CrossRef]
27. Proudman, J. *Dynamical Oceanography*; Methuen: London, UK, 1953.
28. Hervouet, J.-M.; Denis, C.; David, E. Revisiting the Thompson boundary conditions. In Proceedings of the XVIIIth Telemac & Mascaret User Club 2011; Hervouet, J.-M., Razafindrakoto, E., Denis, C., Eds.; EDF R&D: Chatou, France, 2011; pp. 142–147.